Histol Histopath (1993) 8: 73-82

Histology and Histopathology

Ultrastructural substrates for increased lung water content in experimental pulmonary edema

H. Oda[1], M. Arakawa[1], K. Kambara[1], K. Nakahara[1], T. Segawa[1], F. Ando[1], T. Kawada[1], S. Hirakawa[1], S. Shoumura[2] and H. Isono[2]

[1]Second Department of Internal Medicine and [2]First Department of Anatomy, Gifu University School of Medicine, Gifu 500, Japan

Summary. We examined the relationship between the incidence of ultrastructural changes in the alveolar septum and the extravascular lung water content. Pulmonary edema was induced in 18 mongrel dogs by either dextran (n=12) or alloxan (n=6) administration. Six other dogs served as controls. Extravascular lung water content was measured by the thermal-dye double indicator dilution method. Specimens of lung tissue were examined with an electron microscope, and the incidence of 13 types of pathological changes in the alveolar septum was studied. For each type of pathological change, the incidence was correlated with the magnitude of lung water content. The following results were obtained. The incidence of edematous changes in the alveolar interstitium (widening of the interstitial space, and dispersion and disarray of collagen fibres in the interstitial space) was well correlated with lung water content ($r=0.78$, $p<0.01$, and $r=0.84$, $p<0.01$, respectively). The correlation was not significant in the remaining types of changes. We conclude that the incidence of the pathological changes in the alveolar septum is increased along with the increase in the content of lung water in both dextran- and alloxan-induced experimental pulmonary edema in dogs.

Key words: Pulmonary edema, Dextran-induced edema, Alloxan-induced edema, Electron microscopy, Extravascular lung water

Introduction

Pulmonary edemas is defined as «a pathological state in which there is abnormal extravascular water storage in the lung» (Visscher et al., 1956). For the quantitative evaluation of the pulmonary edema, several methods have been applied (Staub, 1974). The double indicator dilution method using heat as a diffusible indicator might be, in particular, a promising clinical tool for measuring lung water content (Lewis et al., 1979; Noble et al., 1980; Mihm et al., 1982; Yasuda et al., 1984; Arakawa et al., 1985; Kambara et al., 1985; Iinuma et al., 1986). It is worthwhile to compare these measurements of lung water level with the morphological changes of the alveolar septum (Staub and Hogg, 1980), although the alveolar septum is the second portion in which extravascular lung water accumulates following the peribronchovascular spaces. However, to our knowledge, there are few reports which correlate the lung water measurements with the pathological changes in pulmonary edema, especially ultrastructural changes in the alveolar septum (Noble et al., 1974).

In the present study, we produced experimental pulmonary edema (increased-pressure or increased-permeability edema) in dogs and correlated extravascular lung water content, measured by the double indicator dilution method, with the incidence of ultrastructural changes in the alveolar septum. The incidence of the changes was semiquantitatively determined as described in the previous studies from our laboratory (Kitamura et al., 1985; Nakahara et al., 1988).

Offprint requests to: Dr. Hiroshi Oda, M.D., Department of Cardiology, Prefectural Gifu Hospital, 4-6-1 Noisshiki, Gifu-shi, Gifu 500, Japan

Materials and methods

Experimental protocol

Twenty-four adult mongrel dogs of either sex weighing between 8 and 18 kg (mean, 12.4 kg) were used; 18 dogs with pulmonary edema and 6 dogs in control state. The dogs were anaesthetized with an intravenous injection of sodium pentobarbital (25 mg/kg), intubated, and allowed to breathe spontaneously. When the above-described preparations had been completed, baseline levels of extravascular lung thermal volume (EVLTV) were obtained by the double indicator dilution method using heat and indocyanine green, which will be described in detail later. We randomly produced graded levels of increased-pressure or

increased-permeability pulmonary edema and divided dogs into four groups. Six control dogs were kept untreated for 30 minutes (Group C). Six dogs received 100 ml/kg of dextran-70 (Macrodex, Pharmacia AB) intravenously for 30 minutes (Group D-30), and six other dogs received 100ml/kg of dextran-70 and then were kept in observation for 60 minutes to produce severer pulmonary edema (Group D-90). Six dogs received 100 mg/kg of alloxan (alloxan monohydrate, Kishida Chemical Co.) intravenously in bolus and were kept in observation for 30 minutes without further intervention (Group A). After the final measurement of EVLTV had been completed, dogs were killed with a bolus intravenous injection of KCl. Within minutes, the lungs were removed from the thorax in an inflated condition, and samples of lung tissue were excised from the surface of the right lower lobe where pulmonary edema appeared severe at macroscopic level.

Electron microscopic studies

Each samples collected for electron microscopic study was cut into 1 mm cubes that were fixed in 2.5% glutaraldehyde in 0.1M cacodylate buffer at pH 7.4 for one hour. The samples were then postfixed in 1% OsO_4 for two hours, dehydrated in a graded ethanol series and embedded in Epon 812. Thin sections were cut using glass knives on an LKB ultramicrotome, stained with uranyl acetate and lead citrate, and examined with a Hitachi HS-8 transmision electron microscope.

About 40 electron micrographs were taken from each dog in four groups without prior knowledge of the experimental intervention, and 20 electron micrographs (final magnification, x 4,700 - 10,000) were chosen for each dog with caution to meet the quality of micrographs for the examination of the alveolar septum.

Table 1. Electron microscopic pathological patterns.

1	Erythrocytes within the alveoli.
2	Fibrin within the alveoli.
3	Swelling of epithelial cells.
4	Increase of epithelial cellular vesiculation.
5	Epithelial cellular vacuolization.
6	Swelling of endothelial cells.
7	Increase of endothelial cellular vesiculation.
8	Endothelial cellular vacuolization.
9	Widening of the interstitial space.
10	Dispersion and disarray of collagen fibres.
11	Erythrocytes in the interstitial space.
12	Focal disruption of epithelial cellular continuity.
13	Subendothelial blister.

A total of 480 micrographs from 24 dogs were serially numbered and then randomly mixed by shuffling, so that we could examine these micrographs further in a blind fashion. We examined electron micrographs on 13 electron microscopic pathological patterns (Table 1) which were frequently documented in earlier ultrastructural studies on pulmonary edema (Finegold, 1967; Cottrell et al., 1967; Pietra et al., 1969; Hurley, 1977; Pietra, 1978; Wysolmerski et al., 1984; Durham et al., 1985; Montaner et al., 1986). We gave a plus if pathological pattern was clearly present, and a minus if pathological pattern was not clearly present. Thereafter, the incidence of each of the 13 pathological patterns was determined in each dog. To observe the correlation, this incidence (Y axis) was plotted against the final EVLTV of dogs (X axis).

Extravascular lung water determinations

Extravascular lung water was measured as EVLTV by

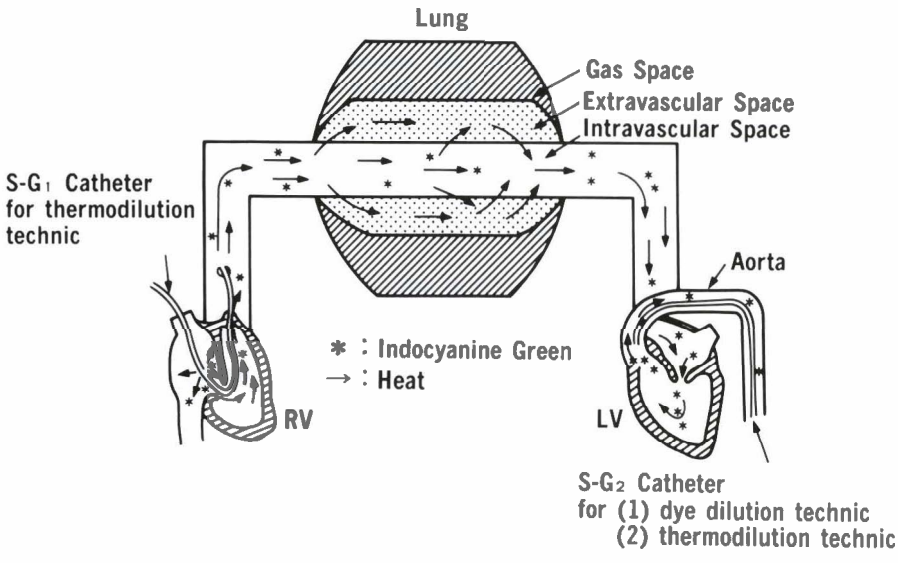

Fig. 1. Schematic presentation of the thermal-dye double indicator dilution method. Indocyanine green dye remains in the vascular space, while heat diffuses into the extravascular space and returns. A Swan-Ganz cathether (S-G_1 catheter) with a thermister on its tip is positioned in the pulmonary artery trunk. Another Swan-Ganz catheter (S-G_2 catheter) with a thermister on its tip, and a Sones catheter are positioned in the aortic root.

thermal-dye double indicator dilution method, which has been described in detail elsewhere (Yasuda et al., 1984; Arakawa et al., 1985; Kambara et al., 1985; Iinuma et al., 1986). Briefly, 5 ml of ice-cold indocyanine green solution was rapidly injected in a bolus into the right atrium through a Swan-Ganz catheter (93A-431H-7.5F, Edwards Laboratories Inc.). The thermodilution curve was recorded by cardiac output computer (Model 9520, American Edwards Laboratories) through the other Swan-Ganz catheter located in the aortic root, and the dye-dilution curve was recorded by constant withdrawal of blood (Model D-014, Lyons Medical Instrument Corporation) from the aortic root. The EVLTV was calculated as a product of cardiac output and the difference in mean transit times between the thermodilution curve and dye-dilution curve, both of which were manually calculated (Fig. 1). This EVLTV includes the thermally equilibrated volume with solid tissue in the lung and with the left ventricular wall. Based on our study, the relation of EVLTV to blood-free weighed lung water (WLW) yielded an equation, EVLTV = 1.16 x WLW +0.03 ($r=0.93$, $p<0.001$), indicating that EVLTV overestimated WLW by about 20% (Yasuda et al., 1984).

Statistical analysis

Values are expressed as means ± SD. For the analysis of correlation between EVLTV and the incidence of pathological patterns, linear regression equations were calculated using a least-squares method. When necessary, non-linear regression equation was obtained using iterative least-squares curve-fitting method. For both methods, the coefficient of correlation was calculated. A probability value (p) less than 0.05 was considered significant.

Results

Extravascular lung water

Baseline values of EVLTV were not statistically different among each groups. Final values of EVLTV were significantly increased from baseline values in experimental groups, and mean of values of EVLTV in Group D-90 was higher than those in Group A. The final values ranged widely from 5.6 ml/kg to 22.3 ml/kg (Table 2).

Table 2. Physiological data.

		EVLTV (ml/kg)*	
Group**	n	Range	Mean±SD
Group C	6	5.6-7.8	6.3±0.8
Group A	6	9.9-14.9	12.4±2.0
Group D-30	6	10.4-22.3	15.9±4.5
Group D-90	6	13.5-21.7	18.0±3.6
Total	24	5.6-22.3	13.1±5.2

*Extravascular lung thermal volume (EVLTV) obtained immediately before their sacrifice. **Group C, control group; Group A, alloxan group; Group D-30, dextran group observed for 30 minutes; Group D-90, dextran group observed for 90 minutes.

Correlations between extravascular lung water and the incidence of ultrastructural changes

We summarize correlations between extravascular lung water and the incidence of ultrastructural changes as follows (Figs. 2, 3). Ultrastructure of alveolar septum in a control dog is shown in Figure 4.

1. Erythrocytes within the alveoli (Fig. 5): Although there was an overall positive correlation between EVLTV and the incidence of this finding ($Y=1.50X-4.18$, $r=0.412$, $p<0.05$), the incidence was very low in Group A (alloxan-induced edema) (Fig. 2A).
2. Fibrin within the alveoli (Fig. 6): There was no significant correlation ($0.05<p<0.10$) (Fig. 2B).
3. Swelling of epithelial cells (Fig. 7): There was no significant correlation ($p>0.10$). Although this pathological pattern was virtually limited to Group A (alloxan-induced edema), there was no correlation even when limited to Group A (Fig. 2c).
4. Increase of epithelial cellular vesiculation: There was no significant correlation ($p>0.10$). there was no specific difference between the four groups as to this finding (Fig. 2D).
5. Epithelial cellular vacuolization (Figs. 6, 7): There was no significant correlation ($p>0.10$). There was no specific difference between the four groups (Fig. 2E).
6. Swelling of endothelial cells (Fig. 7): There was no significant correlation ($p>0.10$). This pathological pattern appeared more frequently in Group A than in Group D-30 or Group D-90 (Fig. 2F).
7. Increase of endothelial cellular vesiculation: There was no significant correlation ($p>0.10$). There was no specific difference between the four groups (Fig. 2G).
8. Endothelial cellular vacuolization (Fig. 7): There was no significant correlation ($p>0.10$) (Fig. 2H).
9. Widening of the interstitial space (Figs. 8, 9): There was positive linear correlation between EVLTV and the incidence of this pathological finding ($Y=4.27X-5.57$, $r=0.775$, $p<0.01$) (Fig. 3A). A better fit between two variables was expressed with an exponential function ($Y=100(1-1.70e^{-0.110X})$, $r=0.871$, $p<0.01$) (Fig. 3B).
10. Dispersion and disarray of collagen fibres (Figs. 8, 9): This finding showed positive correlation with EVLTV ($Y=4.60X-8.30$, $r=0,837$, $p<0.01$) (Fig. 3C). A better fit between two variables was expressed with an exponential function ($Y=100(1-1.85e^{-0.117X})$, $r=0.906$, $p<0.01$) (Fig. 3D).
11. Erythrocytes in the interstitial space (Fig. 10): There was a positive, but rough, overall correlation between EVLTV and the incidence of this pathological change ($Y=1.06X-6.10$, $r=0.561$, $p<0.01$). Interestingly this pathological finding was virtually confined to Group D-30 or Group D-90 (dextran-induced edema)

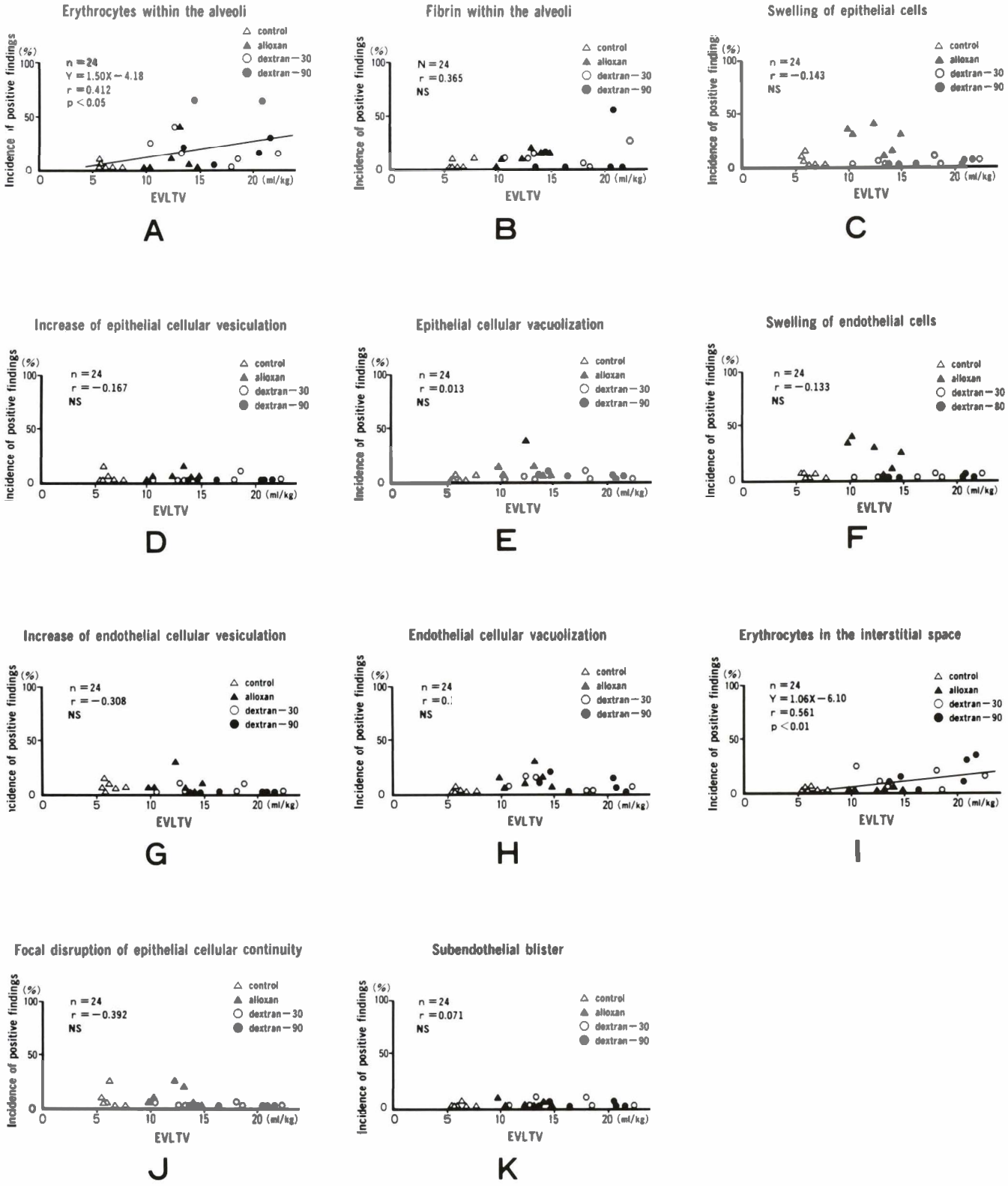

Fig. 2. A set of figures showing relationships between incidence of 11 specific items of ultrastructural pathological changes at the alveolar septum and extravascular lung thermal volumes (EVLTV). In **B**, **C**, **D**, **E**, **F**, **G**, **H**, **J** and **K**, there is no correlation between incidence of the specific item of ultrastructural pathological change and extravascular lung thermal volume. In **A** and **I**, there are rough linear correlations between incidence of the findings and extravascular lung thermal volume.

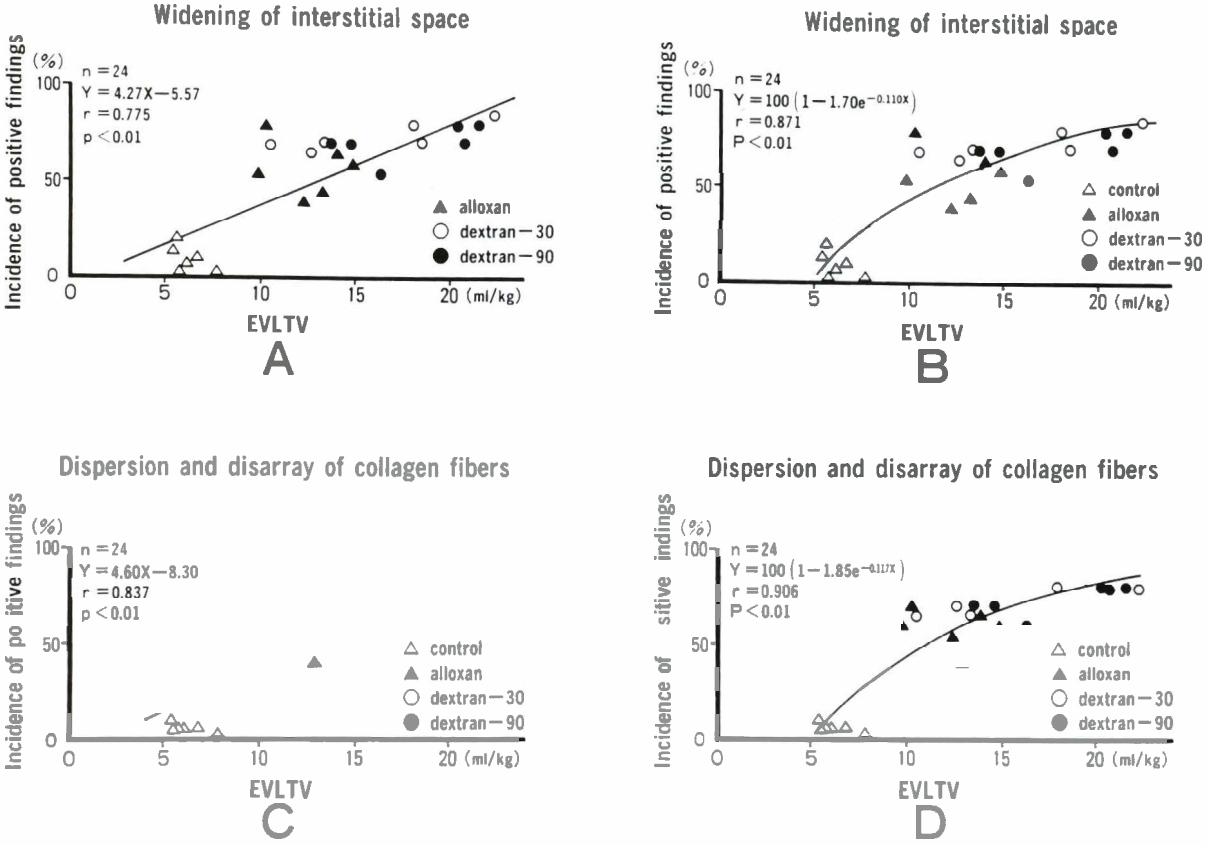

Fig. 3. A set of figures showing relationships between incidence of two items of ultrastructural pathological changes at the alveolar septum and extravascular lung thermal volumes (EVLTV). In **A** and **C**, a linear correlation is found between incidence of pathological change and EVLTV. In **B** and **D**, a better fit between two variables is expressed with an exponential function.

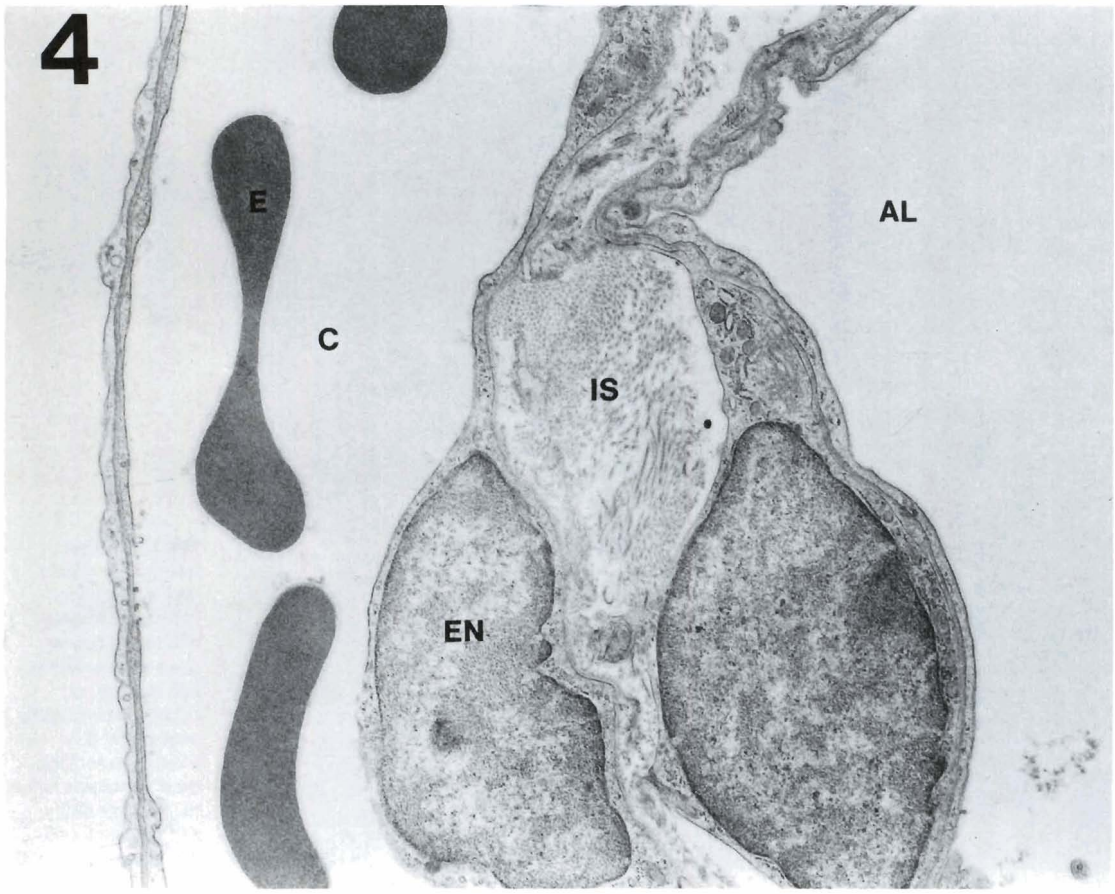

Fig. 4. Electron micrograph of the alveolar septum in a control dog (Group C) with extravascular lung thermal volume of 5.7 ml/kg, showing normal interstitial space (IS).
E: erythrocyte,
C: capillary,
EN: endothelial cell,
AL: alveolus.
x 10,000

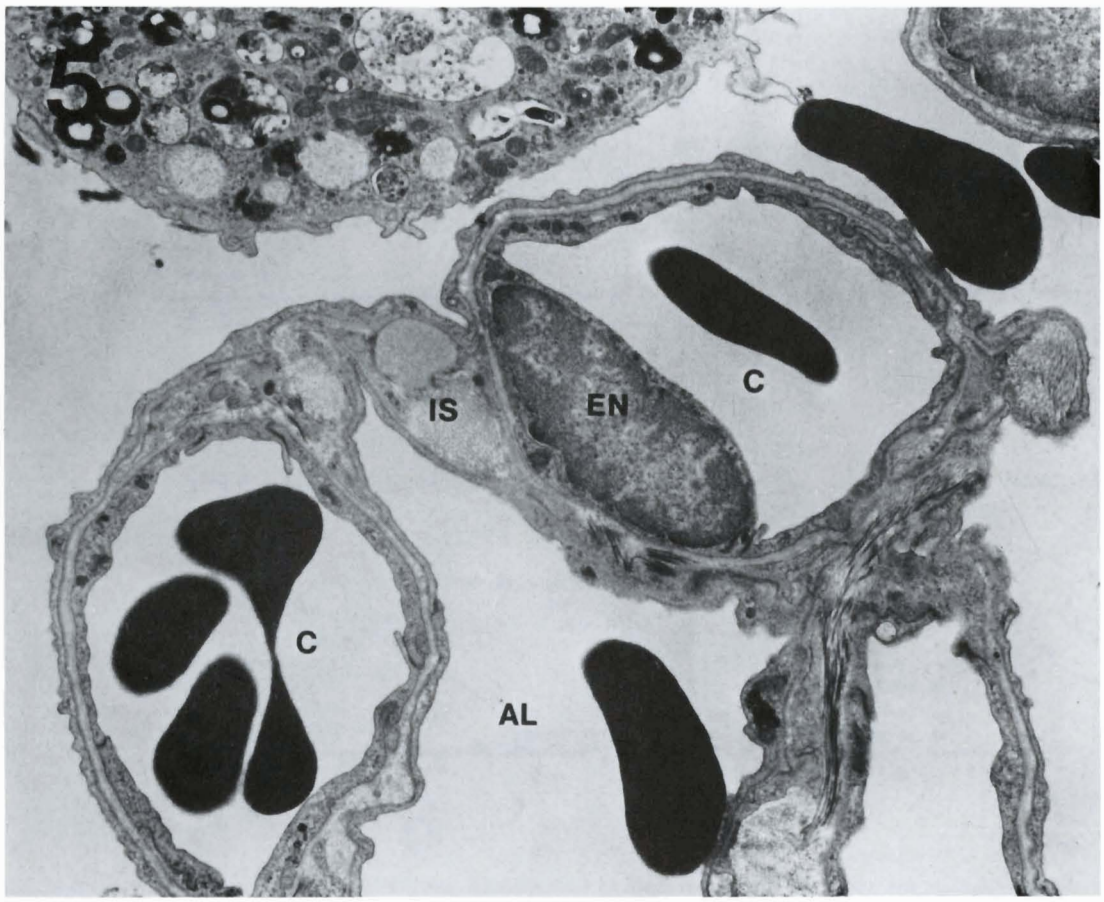

Fig. 5. Electron micrograph from a dog with dextran-induced pulmonary edema (Group D-30) showing erythroyctes within the alveolus (AL). Extravascular lung thermal volume was 12.7 ml/kg. C: capillary, IS: interstitial space, EN: endothelial cell. x 7,500

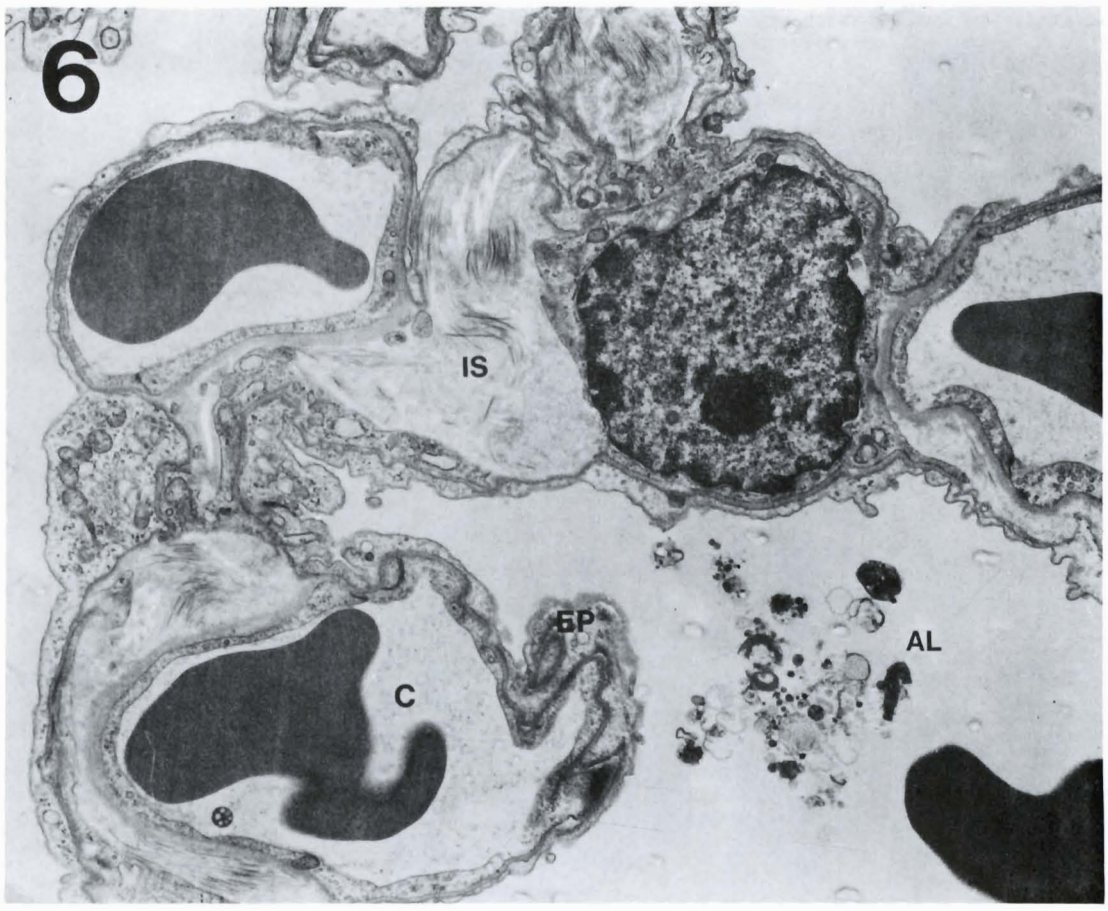

Fig. 6. Electron micrograph from a dog with alloxan-induced pulmonary edema (Group A), showing dispersion and disarray of collagen fibres in the interstitium (IS). Extravascular lung thermal volume is 9.9 ml/kg. C: capillary, EP: epithelial cell, AL: alveolus. x 7,500

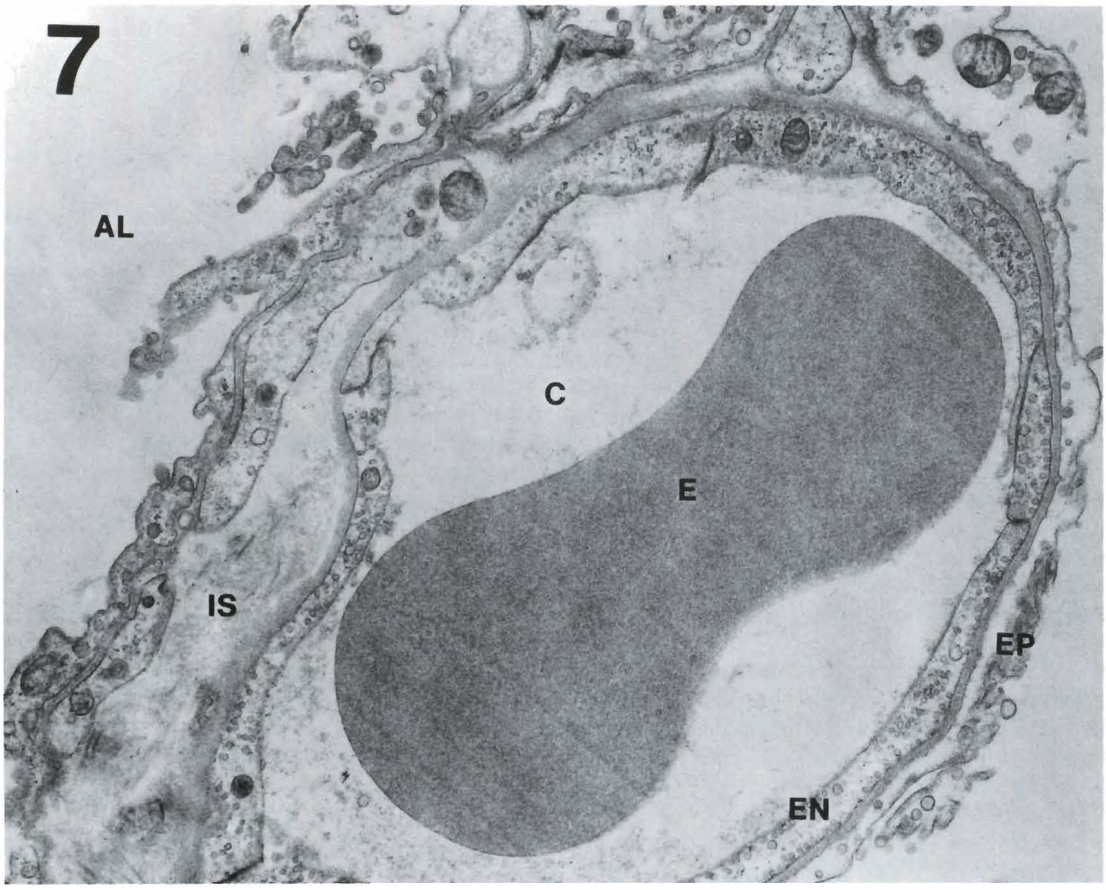

Fig. 7. Electron micrograph from a dog with alloxan-induced pulmonary edema (Group A), showing dispersion and disarray of collagen fibres, swelling and vacuolization of epithelial (EP) and endothelial cell (EN), and disruption of epithelial cell. Extravascular lung thermal volume is 9.9 ml/kg. C: capillary, E: erythrocyte, IS: interstitial space, AL: alveolus. x 12,000

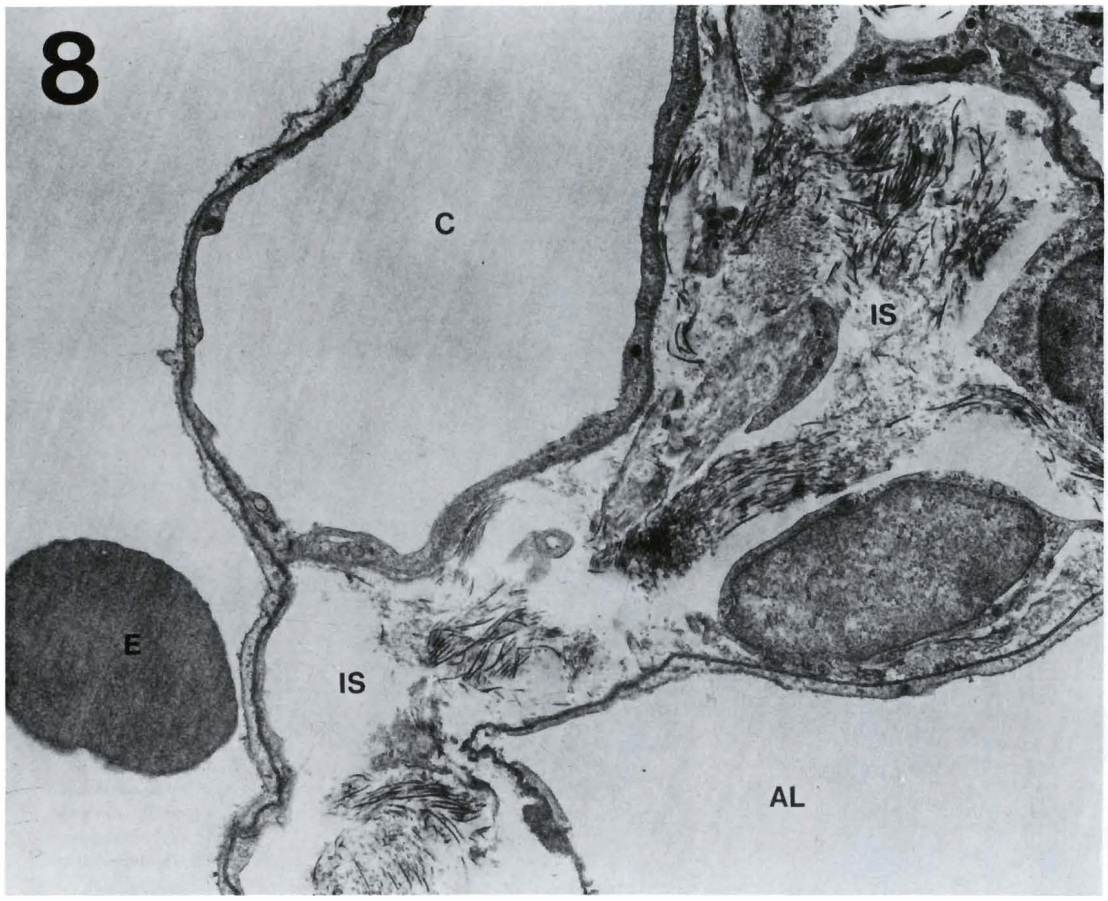

Fig. 8. Electron micrograph from a dog with dextran-induced pulmonary edema (Group D-30), showing widening of interstitial space (IS) and the dispersion and disarray of collagen fibres. Extravascular lung thermal volume is 18.0 ml/kg. E: erythorycte, C: capillary, AL: alveolus. x 7,500

(Fig. 2I).

12. Focal disruption of epithelial cellular continuity (Fig. 7): There was no significant correlation ($p>0.10$). There was no specific difference between the four groups (Fig. 2J).

13. Subendothelial blister: This finding was seldom detected in any group, and there was no significant correlation ($p>0.10$) (Fig. 2K).

Discussion

We have previously reported about a fine interobserver and intraobserved reproducibility in the semiquantitative evaluation of the incidence of ultrastructural changes (Kitamura et al., 1985), and have found the distinctive ultrastructural characteristics of alloxan-induced or dextran-induced pulmonary edema (Nakahara et al., 1988).

In the present study, we examined whether some of the 13 ultrastructural pathological findings showed significant correlation with extravascular lung water measured with the thermal-dye technique (EVLTV). The widening of the interstitial space, and the dispersion and disarray of collagen fibres, both of which probably express the alveolar interstitial edema, are the changes that are positively correlated with EVLTV, with high coefficient of correlation, when all data from each of the groups were combined.

For induction of pulmonary edema we used two agents in which the mechanism was different: dextran increases lung water mainly by raising the pulmonary microvascular pressure; and alloxan inceases lung water mainly by increasing the microvascular permeability. However, the incidence of these morphological changes, suggesting interstitial edema at the alveolar septum, was similar at the corresponding level of EVLTV between the two different types of pulmonary edema. This fact probably indicates a similar distribution pattern of accumulated lung water in these two groups, but not necessarily the same sequence of lung water accumulation. In short, these pathological findings represent not the serial change of lung water accumulation but the final stage of pulmonary edema. We presently restricted the extent of examination to the alveolar septum, simply because of the technical difficulty in studying the peribronchovascular spaces with an electron microscope.

Staub et al. (1967) defined, in their classic study, the sequence of fluid accumulation in experimental pulmonary edema by means of light microscopy. They stated that fluid appears first in the peribronchovascular connective tissue space and then in the connective tissue

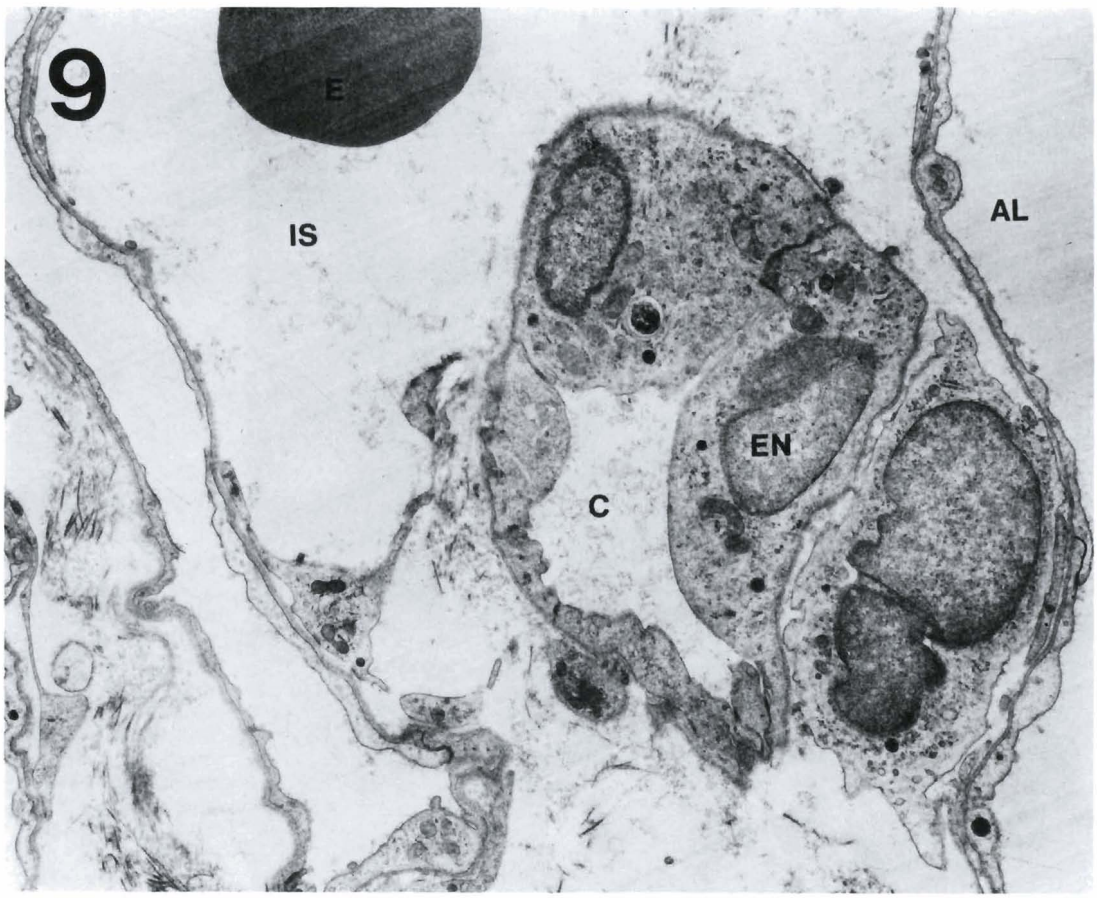

Fig. 9. Electron micrograph from a dog with dextran-induced pulmonary edema (Group D-90), showing markedly enlarged interstitium (IS) and dispersion and disarray of collagen fibres. Extravascular lung thermal volume is 21.7 ml/kg. C: capillary, E: erythorocyte, EN: endothelial cell, AL: alveolus. x 7,500

space of the alveolar septum, and finally in the alveolar space (alveolar flooding). They also showed that as edema progresses, alveolar wall thickness increases correspondingly. Examining in detail the distribution of edema fluid in bronchoalveolar bundles in dogs with permeability edema, Michel et al. (1984) demonstrated that edema fluid accumulates preferentially in the loose periarterial interstitium and less preferentially in the bronchiolar and bronchial interstitium. Bongard et al. (1984) attempted to clarify the relationship between lung morphometrics and lung water content, measured with the thermal-green dye technique. They found that the perivascular cuff width ratio to vessel diameter correlates positively and linearly with lung water content, and alveolar flooding begins when lung water content doubles from normal. However, their morphological investigation was performed by photographing random sections of the lungs while still frozen, and ultrastructural changes at the alveolar septum were not examined. Our results suggest that an increase in alveolar wall thickness results primarily from the widening of alveolar interstitium, which is, however, sporadic in early stages of pulmonary edema but becomes «diffuse» as the grade of pulmonary edema progresses.

Ultrastructural changes significantly, but less prominently correlated with lung water

The incidence of appearance of erythrocytes within the alveolar or interstitial spaces showed significant, but less prominent, correlation with EVLTV. Previously we described that this ultrastructural change is almost exclusively limited to dextran-induced pulmonary edema, even though the incidence is rather low even in the dextran group (Nakahara et al., 1988). This is probably because alveolar flooding occurs as a sporadic rather than diffuse phenomenon in the early stage of pulmonary edema (Staub et al., 1967).

Ultrastructural changes not correlated with lung water

Cytopathological changes of epithelial or endothelial cells, such as the increase of vesicles, vacuolization or cell swelling were not correlated with EVLTV. As we have showed previously, these pathological findings are characteristic of alloxan-induced pulmonary edema (Nakahara et al., 1988). This contradictory result may indicate that the cytotoxic changes caused by alloxan administration are not necessarily in parallel with the extent of lung water increase, depending on factors such as dehydration or hemodynamic alteration in the animal.

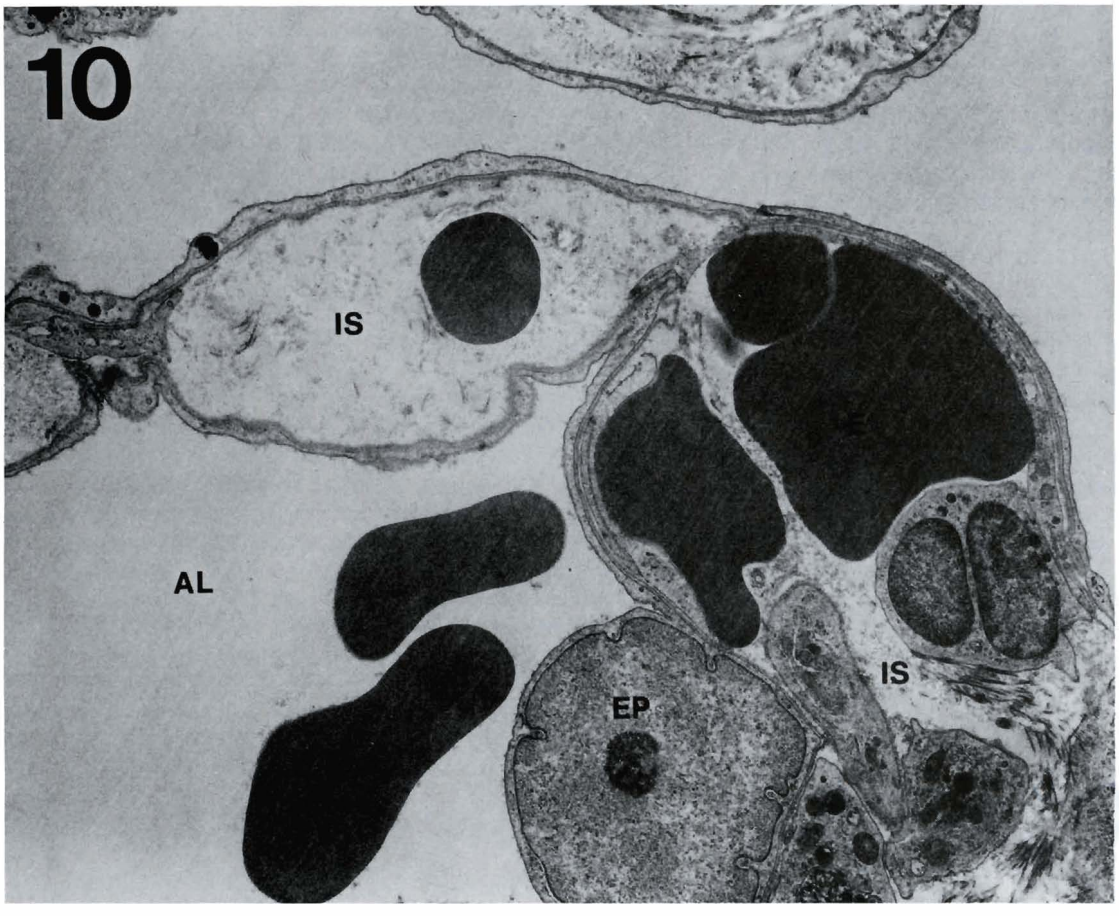

Fig. 10. Electron micrograph from a dog with dextran-induced pulmonary edema (Group D-30), showing widening of interstitial space (IS) with erythrocytes (E) in it. Extravascular lung thermal volume is 18.0 ml/kg. AL: alveolus, EP: epithelial cell. x 7,500

Limits of the present study

The anatomical investigation of the lung in this study was limited to the alveolar level, in disregard of peribronchovascular interstitium which is known to accumulate extravascular water to a considerable extent before the swelling of the alveolar septum. Although it is still controversial whether or not thermal diffusion into the peribronchovascular interstitium and/or alveolar space is sufficient enough to fully detect extravascular thermal volume, EVLTV consists of equilibrated volume with true extravascular lung water, solid tissue in the lung, and with the cardiovascular wall. Accordingly, a simple comparison of the morphological changes at the alveolar level with EVLTV may not be totally satisfactory. Moreover, alveolar septal morphological changes potentially arrive at the plateau, even though extravascular lung water is still increasing by accumulation of extravascular water in the alveolar spaces.

As previously described, the pathogenesis and the ultrastructural alterations were different between dextran- and alloxan-induced pulmonary edema. Furtheremore, the variation in observation period after dextran infusion (30 minutes in one group and 90 minutes in the other group) may produce different morphological changes even in the same intervention by dextran administration. Therefore, these different forms of pulmonary edema may distort the interpretation of morphological changes in relation to extravascular lung water volume.

To overcome these problems, additional studies may be required which should take into account the analysis of time sequence in edema formation and the observation of peribronchovascular space.

References

Arakawa M., Yasuda Y., Kambara K., Iinuma J., Miyazaki H., Yamaguchi M., Takaya T., Nagano T., Goto M., Suzuki T., Tanaka T., Miyamoto H. and Hirakawa S. (1985). Pulmonary blood volume and pulmonary extravascular water volume in men. Jpn. Circ. J. 49, 475-486.

Bongard F.S., Matthay M., Mackersie R.C. and Lewis F.R. (1984). Morphologic and physiologic correlates of increased extravascular lung water. Surgery 96, 395-403.

Cottrell T.S., Levine O.R., Senior R.M., Wiener J., Spiro D. and Fishman A.P. (1967). Electron microscopic alterations at the alveolar level in pulmonary edema. Circ. Res. 21, 783-797.

Durham S.K., Boyd M.R. and Castleman W.L. (1985). Pulmonary endothelial bronchiolar lesions induced by 4-ipomeanol in mice. Am. J. Pathol. 118, 66-75.

Finegold M.J. (1967). Interstitial pulmonary edema. Lab. Invest. 16, 912-924.

Hurley J.V. (1977). Current views on the mechanisms of pulmonary oedema. J. Pathol. 125, 59-79.

Iinuma J., Arakawa M., Yasuda Y., Kambara K., Miyazaki H., Segawa T. and Hirakawa S. (1986). Fluid volume balance between pulmonary intravascular space and extravascular space in dogs. Jpn. Circ. J. 50, 818-828.

Kambara K., Yasuda I., Iinuma J., Arakawa M. and Hirakawa S. (1985). A problem intrinsic to the measurements of the pulmonary extravascular water volume by the thermal-dye technic with the sampling site in the bifurcation of the aorta. Thermal equilibrium with the aortic wall. Jpn. Circ. J. 49, 301-310.

Kitamura Y., Shoumura S., Isono H., Nakahara K., Oda H., Yasuda Y. and Hirakawa S. (1985). Basic study on the incidence of the ultrastructural changes in the experimental pulmonary edema, with special reference to the ultrastructural changes in non-treated dogs. Acta. Sch. Med. Univ. Gifu 33, 1005-1020 (in Japanese).

Lewis F.R., Elings V.B. and Sturm J.A. (1979). Bedside measurement of lung water. J. Surg. Res. 27, 250-261.

Mihm F.G., Feeley T.W., Rosenthal M.H. and Lewis F. (1982). Measurement of extravascular lung water in dogs using the thermal-green dye indicator dilution method. Anesthesiology 57, 116-122.

Michel R.P., Smith T.T. and Poulsen R.S. (1984). Distribution of fluid in bronchovascular bundles with permeability lung edema induced by alpha-naphthyltiourea in dogs. A morphometric study. Lab. Invest. 51, 97-103.

Montaner J.S.G., Tsang J., Evans K.G., Mullen J.B.M., Burns A.R., Walker D.C., Wiggs B. and Hogg J.C. (1986). Alveolar epithelial damage. J. Clin. Invest. 77, 1786-1796.

Nakahara K., Arakawa M., Kambara K., Oda H., Hirakawa S., Shoumura S. and Isono H. (1988). Electron microscopic pathological patterns of alveolar septum in acute dextran-induced and alloxan-induced pulmonary edema in dogs. Histol. Histopath. 3, 395-404.

Noble W.H., Kovacs K. and Kay J.C. (1974). Fine structural changes in haemodynamic pulmonary oedema. Can. Anaesth. Soc. J. 21, 275-284.

Noble W.H., Kay J.C., Maret K.H. and Caskanette G. (1980). Reappraisal of extravascular lung thermal volume as a measure of pulmonary edema. J. Appl. Physiol. 48, 120-129.

Pietra G.G., Szidon J.P., Leventhal M.M. and Fishman A.P. (1969). Hemoglobin as a tracer in hemodynamic pulmonary edema. Science 166, 1643-1646.

Pietra G.G. (1978). The basis of pulmonary edema, with emphasis on ultrastructure. Monogr. Pathol. 19, 215-234.

Staub N.C. (1974). Pulmonary edema. Physiol. Rev. 54, 679-811.

Staub N.C., Nagano H. and Pearce M.L. (1967). Pulmonary edema in dogs, especially the sequence of fluid accumulation in lungs. J. Appl. Physiol. 22, 227-240.

Staub N.C. and Hogg J.C. (1980). Conference report of a workshop on the measurement of lung water. Crit. Care Med. 8, 752-759.

Visscher M.B., Haddy F.J. and Stephens G. (1956). The physiology and pharmacology of lung edema. Pharmacol. Rev. 8, 389-434.

Wysolmerski R., Lagunoff D. and Dahms T. (1984). Ethchlorvynol-induced pulmonary edema in rats. Am. J. Pathol. 115, 447-457.

Yasuda Y., Hirakawa S., Arakawa M., Kambara K. and Iinuma J. (1984). A problem in the measurements of pulmonary extravascular water volume by double indicator dilution method, using heat and dye. Termal diffusion into the left ventricular wall. Jpn. Circ. J. 48, 580-590.

Accepted August 6, 1992